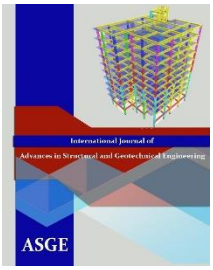

International Journal of Advances in Structural and Geotechnical Engineering

https://asge.journals.ekb.eg/

Print ISSN 2785-9509 *Online ISSN 2812-5142*

Special Issue for ICASGE'19

EFFICIENT STEEL-REINFORCED UHP-SHCC STRENGTHENING FOR LAP-SPLICED RC BEAMS

Emad E. Etman, Ahmed M. Atta, Ahmed T. Baraghith, and Asmaa F. Edris

ASGE Vol. 03 (02), pp. 61-76, 2019

International Conference on Advances in Structural and Geotechnical Engineering

ICASGE'19

25-28March 2019, Hurghada, Egypt

EFFICIENT STEEL-REINFORCED UHP-SHCC STRENGTHENING FOR LAP-SPLICED RC BEAMS

Emad E. Etman[1], Ahmed M. Atta[2], Ahmed T. Baraghith[3], Asmaa F. Edris[4]

[1]*Professor, Faculty of Engineering, Tanta University, Egypt*
E-mail: emad.etman@f-eng.tanta.edu.eg
[2]*Professor, Faculty of Engineering, Tanta University, Egypt*
E-mail: drahmedatta2003@yahoo.com
[3]*Assistant Professor, Faculty of Engineering, Tanta University, Egypt*
E-mail: ahmed_baraghit@yahoo.com
[4]*Master Candidate, Faculty of Engineering, Tanta University, Egypt*
Civil Engineer, Water and Sanitation Company, Tanta, Egypt
E-mail: eng.asma2012@gmail.com

ABSTRACT

This paper investigates the effectiveness of strengthening reinforced concrete (RC) beams with tension lap splices using a jacketing of Ultra High Performance Strain Hardening Cementitious Composites (UHP-SHCC) with embedded vertical stirrups. Nine RC specimens with different lap splice lengths at the mid span region were tested in flexure to examine the performance of the proposed technique for eliminating the bond failure mode in such lap splices. The test parameters were the lap splice length and the effect of confinement (no confinement and a jacketing of UHP-SHCC with embedded stirrups at different spacing). The test results show that, whilst the spliced control specimens failed in a brittle manner due to splitting of main steel, using UHP-SHCC jacketing with embedded vertical stirrups has increased the ultimate load and changed the mode of failure to flexural and ductile one. Moreover, a pronounced effect on increasing the bond strength between the reinforcing steel bars and surrounding concrete was observed for all confined specimens. Consequently, a satisfactory ductility was obtained which confirms the applicability of the UHP-SHCC jacketing for strengthening lap-spliced region of RC beams.

Keywords: Lap splice, Strengthening, UHP-SHCC, Bond strength, Ductility.

1 INTRODUCTION

Splicing of reinforcing bars is one of the common preparations used in concrete structures to connect two bars to have continuous reinforcement bars in concrete elements. There are three methods to carry out splicing; lap splices, welded splices and mechanical splices. The most effective, usual and economical splicing method is lap splicing and it is often achieved by overlapping of two parallel bars with enough length. Lap splicing is divided into contact and non-contact lap splices. Contact lap splices are used frequently because stress transfer from deformed bars to surrounding concrete is mainly through mechanical interlocking of lugs which increase the bond between spliced bars and concrete [1-2]. The main parameters that influence the bond strength between steel reinforcing bars and concrete include type of concrete, concrete cover, the presence of confinement in the form of transverse reinforcement, which can delay and control crack propagation, diameter and geometry of the reinforcing bar and lap splice length [3-6].

As the work on splices requires knowledge about the bond between surrounding concrete and steel rebar, many researchers studied the bonding behavior of tension lap splices in RC members. Transverse reinforcement confines spliced bars by restricting the progression of

splitting cracks, which leads to increasing the bond force required to cause failure [7-9]. Also, using stirrups in the splice region enhanced the ductility [10]. Abdel-Kareem et al. [11] studied the effect of transverse reinforcement on the behavior of tension lap splice in high-strength reinforced concrete specimens. The experimental results showed that the displacement ductility increased and the mode of failure changed from splitting bond failure to flexural failure with increasing the vertical transverse reinforcement in splice region more than 25% that required by ACI 318-05 [12].

Tarabia et al. [13] concentrated on the behavior of spliced reinforced concrete specimens in tension regions. The cut-off ratio, lap splices length, type, spacing and shape of transverse reinforcement in the splice region were investigated. They concluded that, using of transverse reinforcement with lap splice length = 27 d_b (where d_b is the bar diameter), and 100% cut off ratio led to enhancement in ultimate loads and ductility compared to the un-spliced specimen. The bond strength and ductility of lap-spliced RC specimens was investigated by Rakhshanimehr et al. [14], it was found that, a certain minimum amount of transverse reinforcement was needed to achieve a satisfactory ductility response for lap-spliced RC specimens and using of smaller stirrup sizes and spacing resulted in a better ductility response.

Recently, most of the research work has focused on confining deficient lap splices. Various techniques have been developed and used in order to strengthen insufficient lap splices such as; external post tensioning techniques, Fiber Reinforced Polymers (FRP) laminates, as well as Ultrahigh Performance Fiber-Reinforced Concrete (UHPFRC). Twelve simply supported specimens were designed and tested by Helal et al. [15] to examine the effect of confinement with internal steel stirrups or external Post-Tensioned Metal Straps (PTMS). In comparison to unconfined specimens, the PTMS confinement delayed the splitting failure of the lap splices and enhanced the bond strength by 58 %, while the bar slip increased by 80 %.

Furthermore, external confinement using FRP have been used which proven effective at enhancing the bond strength of substandard splices [16-18]. Garcia et al. [19] investigated the strengthening of insufficient lap splices in RC beams using different confinement techniques (internal steel stirrups or external Carbon Fiber Reinforced Polymer (CFRP) sheets). The results of this research indicated that, the use of externally bonded CFRP confinement delayed the splitting failure of the laps and enhanced the bond strength and bar slip up to 65% and 14000%, respectively, compared to unconfined specimens. Hamad et al. [20] also studied the bond strength of tension lap splices in high-strength concrete specimens strengthened with glass fiber reinforced polymer (GFRP) wraps. The main test variables were the GFRP configuration in the splice region (one strip, two strips, or a continuous strip), and the number of layers of the GFRP wraps placed around the splice region (one layer or two layers). The test results demonstrated that, the GFRP wraps were effective in enhancing the bond strength and ductility tension lap splices, especially when continuous strips were applied over the splice region.

On the other hand, Ultrahigh Performance Fiber-Reinforced Concrete (UHPFRC) has been used as a strengthening technique for tension lap-spliced beams by Dagenais and Massicotte [21]. The strengthening technique consisted of replacing normal concrete in the splice region with UHPFRC. The studied parameters were splice length, bar diameter, repair depth, and bar relative position. They didn't use stirrups in the lap splice region to isolate the contribution of UHPFRC. They found that, failure by splitting in the lap splice region was completely eliminated due to the high tensile strength and energy absorption capabilities of the UHPFRC.

Nowadays, Ultra-High-Performance Strain-Hardening Cementitious Composites (UHP-SHCC) have been used for strengthening or repair concrete members. This material is a new generation of fiber reinforced cementitious composites, which has many advantages on large strain capacity as well as high compressive and tensile strength [22-26]. UHP-SHCC is a composite material comprising a cement-based matrix and short polypropylene fibers with outstanding mechanical performance [27-29]. Fig. 1 shows the tensile behavior of UHP-SHCC compared to ordinary Strain Hardening Cementitious Composites (SHCC) and ordinary Ultra High Performance Fiber Reinforced Concrete (UHPFRC).

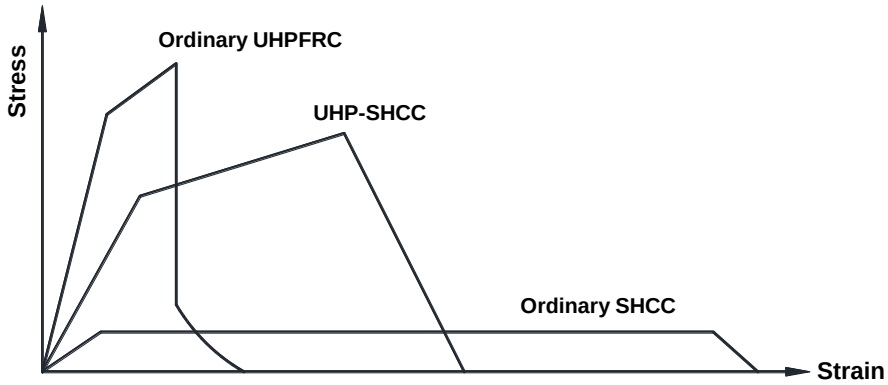

Fig. 1: The tensile behavior UHP-SHCC material compared to that of other materials, (Kunieda et al., 2010).

UHP-SHCC has relatively higher hardening strain compared with ordinary UHPFRC, and relatively higher stress than ordinary SHCC. UHP-SHCC forms a class of cement composites with a tensile stress-strain response that exhibits strain hardening accompanied by multiple cracking. The tensile strength of UHP-SHCC is one of its attractive properties for strengthening reinforced concrete elements, which is significantly larger (twice or more) than that of ordinary SHCC [30-31].

Because of the developed characteristics of the UHP-SHCC material, this paper investigates the effectiveness of UHP-SHCC jacketing with embedded vertical stirrups at enhancing the behavior of tension spliced RC beams in both terms: bond strength and ductility. To achieve this, nine RC specimens were tested in flexure. Four of these specimens were un-confined control with different lap splice lengths and five confined specimens using UHP-SHCC jacketing with embedded vertical stirrups at different spacing in lap splice region. It was found that, the proposed strengthening technique has potential to offer practical and effective solutions to many problems in substandard buildings such as the insufficient or deficient lap splices.

2 EXPERIMENTAL PROGRAM

2.1 Test Specimens and Parameters Examined

Nine RC specimens were prepared and tested under flexural four-point bending loads. The tested specimens had a rectangular section of 150 mm width and 300 mm depth. The total span was 3000 mm with center to center span 2700 mm. The distance between the two applied loads was 900 mm to produce a constant moment region in the middle third of the specimen. Special notches were provided at the bottom of each specimen to define the lap length and reveal the main flexural reinforcement for measurements. The main bottom flexural reinforcement consisted of two steel bars of 12 mm diameter spliced at the mid span region; the top specimen reinforcement consisted of two 10 mm bars outside the lap splice region. To prevent premature shear failure, 8 mm vertical stirrups spaced at 100 mm at the shear span were implemented. The splice region was kept free of transverse reinforcement to examine the strength technique contribution. The concrete cover for all tested specimens was 15 mm per side. Fig. 2 illustrates the geometry and reinforcement for all specimens.

Table 1 summarizes the experimental program and the description of each specimen. The tested specimens were divided into two series. The first series (Series 1) consisted of four control RC specimens without confinement. The first one, BC, had no splice but the others, BC55, BC30 and BC20, had spliced steel bars in tension side with different splice length, the reference specimen BC55 was designed with a splice length according to Egyptian code [31] (55 d_b) but other two specimens BC30 and BC20 were designed with insufficient lap splice length (30 d_b and 20 d_b), respectively. The second series (Series 2) consisted of five RC specimens confined with UHP-SHCC jacketing with embedded vertical stirrups at lap splice region. The strengthening scheme of series 2 specimens is shown in Fig. 3.

Table 1: Description of all tested specimens

Specimen		l_p (mm)	Description of tested specimens
Series 1	BC	------	Control specimen without splice
	BC55	660	Control specimen with lap splice length, l_p= 55 d_b
	BC30	360	Control specimen with lap splice length, l_p= 30d_b
	BC20	240	Control specimen with lap splice length, l_p= 20d_b
Series 2	BS55-60	660	Strengthened specimen with lap splice length, l_p= 55 d_b, confined with 20 mm UHP-SHCC jacketing with vertical stirrups ϕ 8@60mm
	BS30-60	360	Strengthened specimen with lap splice length, l_p 30d_b, confined with 20 mm UHP-SHCC jacketing with vertical stirrups ϕ8@60mm
	BS30-72	360	Strengthened specimen with lap splice length, l_p= 30d_b, confined with 20 mm UHP-SHCC jacketing with vertical stirrups ϕ 8@ 72 mm
	BS30-90	360	Strengthened specimen with lap splice length, l_p= 30d_b, confined with 20 mm UHP-SHCC jacketing with vertical stirrups ϕ 8@ 90 mm
	BS20-60	240	Strengthened specimen with lap splice length, l_p= 20d_b, confined with 20 mm UHP-SHCC jacketing with vertical stirrups ϕ 8@60mm

where d_b is the bar diameter in mm and l_p is the splice length in mm.

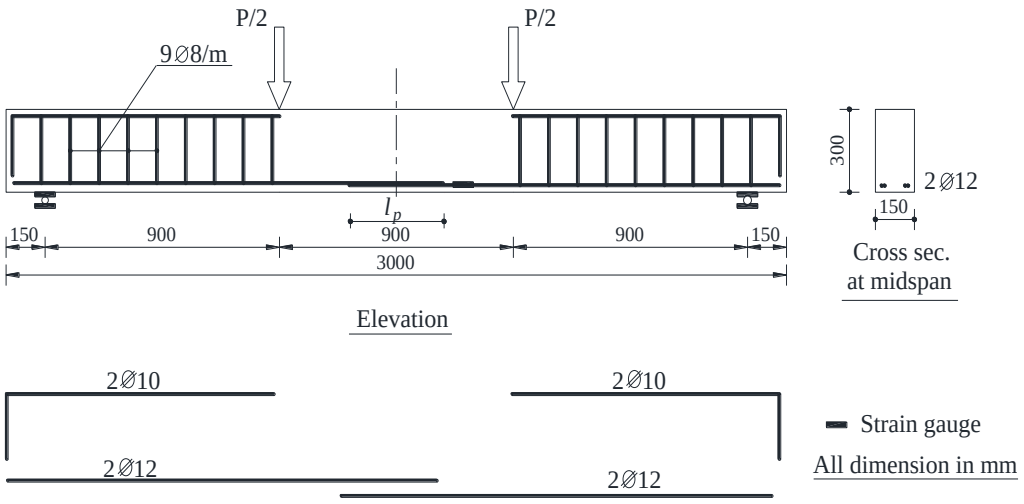

Fig. 2: The tested specimens geometry.

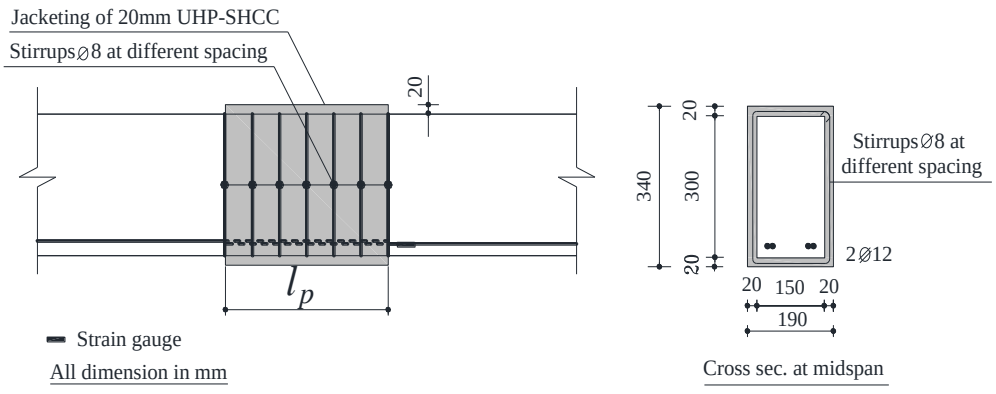

Fig. 3: Strengthening scheme for specimens in series 2.

2.2 Material Properties

The mix proportions of the UHP-SHCC used in strengthening process are listed Table 2. Water to binder ratio (W/B) was 0.20. Ordinary Portland Cement (density: 3.14 g/cm3) was used, and 15% of the design cement content was replaced by silica fume. Quartz sand with diameter less than 0.5 mm was used as a fine aggregate. High strength Polypropylene (PP) fiber was chosen for UHP-SHCC and its volume in mix was 1.5%. The diameter and length of the PP fibers were 0.012 mm and 6 mm, respectively. The mix had design to achieve a compressive strength 60MPa and an ultimate strain of 0.0035. To characterize the compressive properties of the used UHP-SHCC, six standard cubes of size 50 mm were tested at the age of 28 days according to (ASTM C-109, 2008). The averaged compressive strength was determined to be 61.9 MPa. The averaged tensile strength UHP-SHCC was 5.2 MPa. Ready mixed normal strength concrete (NSC) was used to cast all the tested specimens. Table 2 shows the concrete mix proportions by weight for one cubic meter as reported by the supplier. The normal strength concrete mix was designed to achieve an average cube crushing strength after 28 days about 25 MPa. The averaged compressive strength of the used concrete was determined to be 25.8 MPa based on the compressive test results of six cube specimens of size 150mm.

For all specimens, deformed bars having a diameter of 12 mm, 10 mm with nominal yield stress 400 MPa were used for main and secondary reinforcement steel, respectively. Smooth bars having a diameter of 8 mm of nominal yield stress 240 MPa were used for stirrups either in UHP-SHCC strengthening layer or in substrate concrete. Tension tests by the universal testing machine were performed on three specimens for each bar diameter to determine the mechanical properties of the used reinforcement. The actual yield stress for the used deformed bars of 12 mm and 10 mm were 455 MPa and 416 MPa, respectively. For the used 8 mm, the actual yield stress was 255 MPa. The mechanical properties of steel reinforcement are summarized in Table 3. The concrete mix was cast in wooden stiff moulds to prevent any significant movement during placing the concrete. During casting, all specimens were compacted by needle vibrator to ensure consolidation of the concrete mix. All specimens were cured with wet burlap to keep moisture, for seven days and subsequently stored under standard laboratory conditions.

2.3 Strengthening Scheme

Five RC specimens, in series 2, were confined by jacketing of UHP-SHCC with embedded vertical stirrups at the lap splice region. In this technique, the following steps were followed; (1) roughening the surface of specimens at the lap splice region to an average amplitude of about 5 mm by chisel in order to remove slurry cement from external surfaces of coarse aggregates, (2) cleaning the surface of specimens by using a blower, (3) fixing vertical stirrups at lap splice region,(4) coating the strengthened region by epoxy and (5) preparing special wooden formwork for casting UHP-SHCC layer, (6) casting of UHP-SHCC layer, and finally (7) curing the strengthening specimens with wet burlap to keep moisture. Fig. 4 explains the different steps involved in STEEL-REINFORCED UHP-SHCC strengthening technique.

Table 2: Mix proportions of RC and UHP-SHCC material for one cubic meter (kg/m3)

Concrete mix	Cement	Sand	Coarse aggregates	Water	W/B*	Silica fume	Super plasticizers	PP Fiber (6 mm)
RC	350	630	1050	175	0.5	---	---	---
UHP-SHCC	1244	149	---	292	0.2	223	14.9	19.6

* W/B is the water/ binder ratio, B = cement + silica fume

Table 3: Mechanical properties of the steel bars

Bar diameter, mm	Type	Average yield strength, MPa	Average tensile strength, MPa	Average modulus of elasticity, GPa
12	Deformed	455	605	202
10	Deformed	416	594	204
8	Smooth	255	415	203

Fig. 4: Strengthening scheme a) Grinding the surface, b) Formwork, c) Casting of UHP-SHCC, d) Final product of strengthened specimens.

2.4 Instrumentation and Test Set-Up

All specimens were loaded in four point bending scheme using a steel spreader specimen, the loading configuration had a clear span of 2700 mm and a constant moment 900 mm. So, the lap spliced bars in constant moment region were subjected to tension force only as shown in Fig. 5. The specimen was loaded using a manual hydraulic jack by applying downward load and measured by the load cell attached to the jack. Linear Variable Differential Transformers (LVDTs) of sensitivity of 0.01 mm were used to measure vertical deflections at midpoint of the lower specimen soffit. Electrical strain gauges were mounted in reinforcing steel bars as shown in Figs.(2-3) to measure the developed strains. The maximum concrete compressive and tensile strains of the tested specimens were measured using Pi-gauges. An automatic data system was used to monitor loading, displacements and strains. At each load increment, the deformations and strains were recorded.

3 EXPERIMENTAL RESULTS AND DISCUSSION

The test results of all tested specimens are presented and analyzed in order to verify the efficiency of the adopted strengthening techniques in enhancing the bond strength and ductility of tension lap splices. In general, all strengthened specimens achieved higher strength and ductility than that of the control un-strengthened specimens and the mode failure changed from splitting of main steel to flexure failure. As listed in Table 4, the test results are grouped by splice length for control reference and STEEL-REINFORCED UHP-SHCC strengthening specimens and the confinement ratio presented by the spacing between embedded stirrups in UHP-SHCC strengthened layer (60, 72 and 90 mm). Table 5 reports (a) the ultimate load (P_u) of the tested specimens, (b) the cracking load (P_{cr}), and (c) mid-span deflection at ultimate load (Δ_u). The following parts summarize the most significant observations of the experimental programme and discuss the results including modes of failures, load deflection behavior, developed normal strain on spliced steel bars, bond strength as well as the ductility.

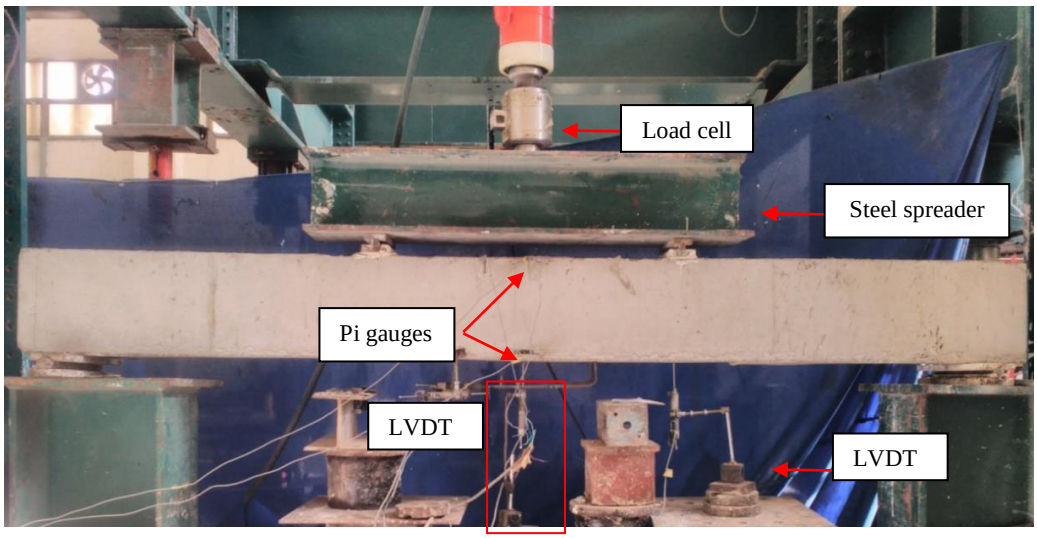

Fig. 5: Test setup

Table 4: Comparison groups

Group	Specimen	Objectiveness
I	BC	Control reference with different lap splice lengths
	BC55	
	BC30	
	BC20	
II	BC	using jacketing of 20 mm UHP-SHCC with vertical stirrups ϕ 8 @ 60 on lap splice region with different lap splice lengths
	BC55	
	BC30	
	BC20	
	BS55-60	
	BS30-60	
	BS20-60	
III	BC	using jacketing of 20 mm UHP-SHCC with vertical stirrups ϕ 8 @ (60 ,72 ,90 mm) on lap splice region as a strengthening technique
	BC30	
	BS30-60	
	BS30-72	
	BS30-90	

3.1 Failure Modes

The cracks were initiated at the soffit specimen section for all control specimens in group (I). As expected, the normal flexural failure was occurred in the reference un-spliced specimen (BC). An extensive yielding of the tension steel reinforcement followed by crushing of concrete in compression region was observed. In the reference spliced specimen BC55 with tension lap splice according to Egyptian code [31], the tension reinforcement also reached the yield strain according the strain monitoring realized during the test. Nevertheless, a brittle failure due to splitting of main steel was occurred. On the other hand, the reference spliced specimens (BC30 and BC20) with insufficient lap splice lengths exhibited a different type of failure mode. Splitting cracks developed suddenly along the splice region and the failure of such specimens was accompanied by loud explosive noise. After failure, nothing prevented the full collapse of these specimens as shown in Fig. 6

The use of UHP-SHCC jacketing with embedded vertical stirrups in the lapped region didn't significantly delay the onset of flexural cracking of the confined specimens. On the contrary to the unconfined specimens, additional flexural cracks appeared at the constant moment region as shown in Fig. 7. Moreover, the mode failure changed from splitting to flexure failure with wide cracks outside the lap splice region. This can be attributed to the gained enhancement from using STEEL-REINFORCED UHP-SHCC strengthening in restricting the splitting cracks and minimizing the width of cracks at lap splice region.

Table 5: Summary of the test results

Specimen	P_{cr} (kN)	P_u (kN)	Δ_u (mm)	Failure mode
BC1	19.4	80.6	13.0	Flexural failure
BC55	19.0	81.3	11.6	Splitting failure*
BC30	18.7	65.6	10.3	Splitting failure
BC20	17.0	47.6	7.3	Splitting failure
BS55-60	20.0	81.0	56.3	Flexural failure
BS30-60	20.0	76.8	53.2	Flexural failure
BS30-72	19.5	74.1	52.7	Flexural failure
BS30-90	19.0	69.7	50.2	Flexural failure
BS20-60	18.0	74.8	52.7	Flexural failure

P_{cr} is the cracking load, P_u is the ultimate load, * refers to that the tension reinforcement reached the yield strain, Δ_u is the displacement at ultimate load.

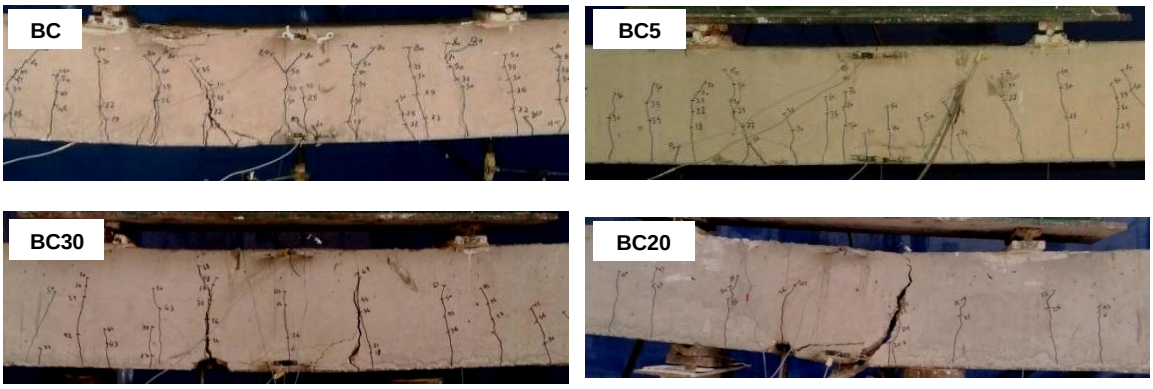

Fig. 6: **Cracks pattern and failure mode of control specimens**

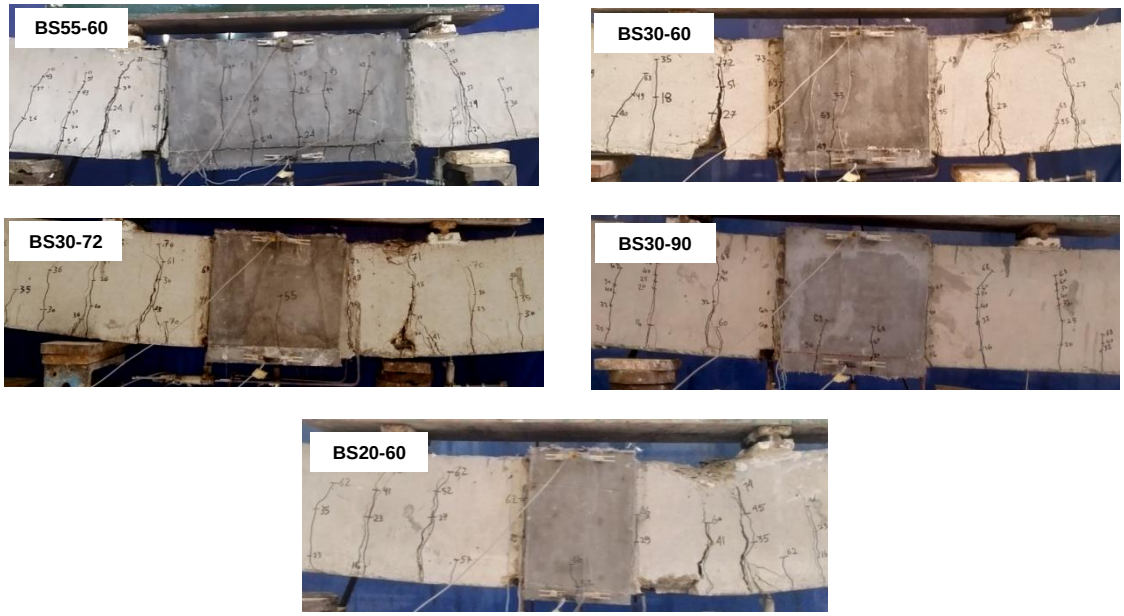

Fig. 7: **Cracks pattern and failure mode of strengthened specimens.**

3.2 Load-Deflection Behavior

Figs. (8a-c) illustrates the load–deflection responses for all the tested specimens. As shown in these figures, the un-spliced reference specimen (BC) showed the elastic and inelastic parts of the load-deflection curve and failed in flexure. Generally, the load–deflection of specimen BC can be classified to three regions; the first region is the initial part of the curve starts from zero loading up to the cracking point. The second region is the post-cracking region, continued up to the yielding point, and finally, the post yield region, up to failure. On contrast, brittle sudden failure was obtained in spliced unconfined specimens (BC55, BC30, and BC20). The initial stiffness of these specimens showed significantly identical behavior at low level of loading up to the cracking load as the concrete cross section for all tested unconfined specimens is the same. After the cracking stage, the spliced unconfined specimens (BC55, BC30 and BC20) showed lower stiffness than the reference un-spliced control specimen (BC), but the relative increase in stiffness between the spliced unconfined specimens (BC55, BC30 and BC20) may be attributed to the extent of the reinforcement with double the cross-sectional area at lap splice region. As shown in Table 5, the maximum capacity of specimens BC30 and BC20 is reduced by 18% and 40%, respectively, compared to the reference un-spliced control specimen (BC) but the spliced specimen BC55 (with sufficient tension lap splice in accordance to the Egyptian code [31]) reached the same capacity of the reference un-spliced specimen (BC).

Comparatively, the load–deflection curves of confined specimens in groups (II) and (III) showed almost the same trend of the load–deflection curve as the reference un-spliced specimen (BC) as shown in Figs. (8b-c). That means, using UHP-SHCC jacketing with embedded vertical stirrups confinement was very effective at improving the load–deflection behavior of confined specimens compared their reference unconfined specimens (BC55, BC30, and BC20).

The confined specimen BS55-60 didn't report any increase in capacity but it showed an increase in deflection at ultimate load by 386% compared to the reference un-spliced specimen (BC55). Meanwhile, the other confined specimens had higher load capacities and larger deflections as shown in Table 5. The ultimate load capacities increased by 18%, 13%, 6%, and 57% and the deflection at ultimate loads increased by 416, 412%, 397, and 620% for specimens BS30-60, BS30-72, BS30-90, and BS20-60, respectively, compared to their reference un-spliced specimens. However, the test results illustrated the efficient of strengthening technique to enhance the load–deflection responses of all confined specimens, but the higher confinement ratios provided by the strengthening technique didn't record an observed change in values at the same lap splice length.

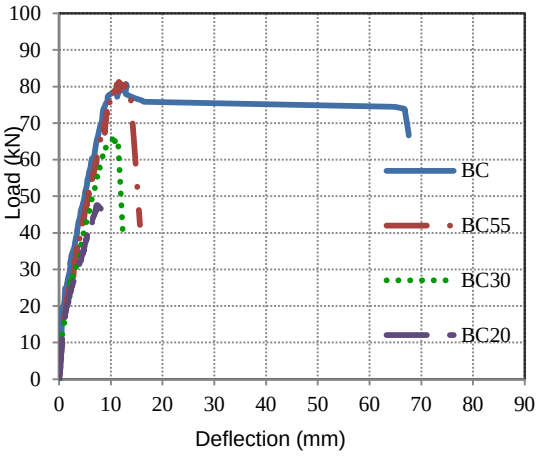

a) Load-deflection behavior for the specimens of group (I).

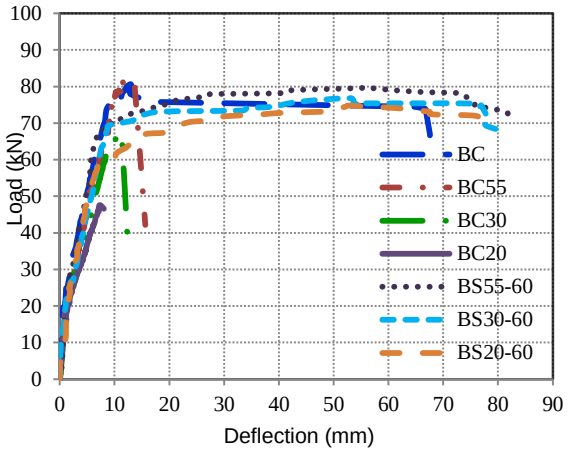

b) Load-deflection behavior for the specimens of group (II).

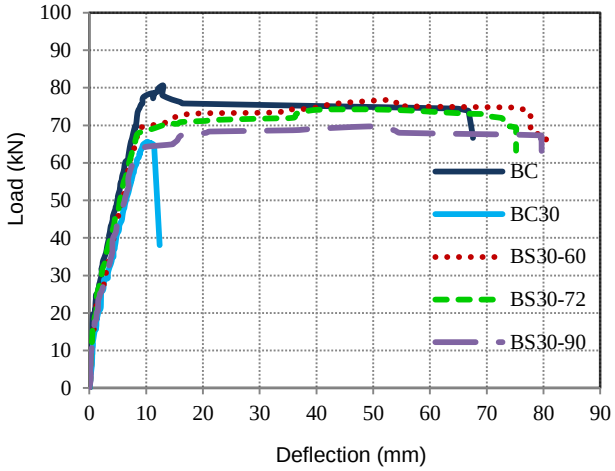

c) Load-deflection behavior for the specimens of group (III).

Fig. 8: Load-deflection behavior for all tested specimens.

3.3 Load-Strain Behavior

Fig. 9a illustrates the load–strain curves for the reference un-spliced specimen (BC) which failed in flexural failure mode. It's obvious that, the relation between the load and strain began liner up to cracking because the concrete was un-cracked and resist all the tensile force resulting from applied load. Once the first crack appeared, all the tensile forces carried by the concrete were transmitted to the main steel. Then, a second linear relation continued up to yield load. Finally, the relation took curve up to failure. On contrary, no yielding was observed in the tensile steel rebar of spliced specimens which resulted in splitting failure.

All strengthened specimens in group (II) and group (III) exhibited yielding of longitudinal steel as indicated in the load–strain relationship depicted in Figs.(9b-c) unlike the reference unconfined specimens in group (I). The strain responses in the spliced steel for the strengthened specimens are significantly similar exceeding yielding of longitudinal steel. The mode of failure changed for the spliced tested specimens from sudden and brittle failure to flexural and ductile failure with yielding of main steel which ensure the efficiency of the used strengthening technique.

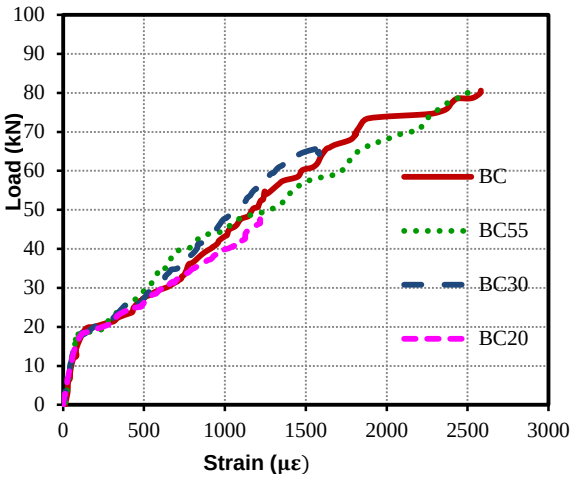

a) Load–strain relationship of main steel for specimens in group (I).

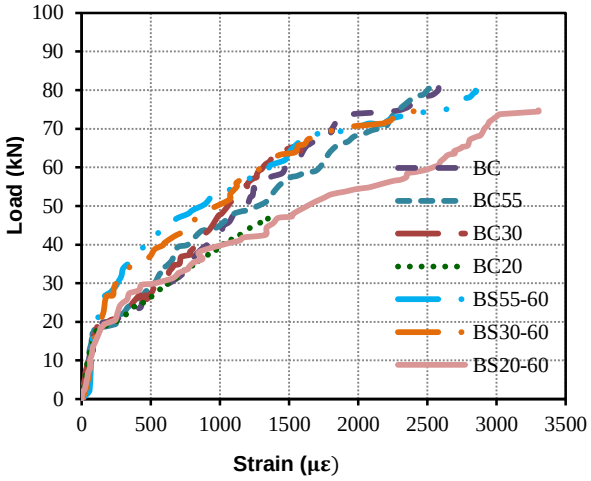

b) Load–strain relationship of main steel for specimens in group (II).

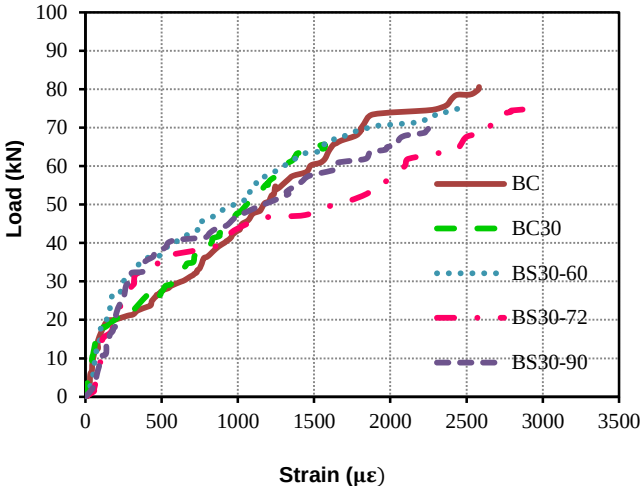

c) Load–strain relationship of main steel for specimens in group (III).

Fig. 9: Load–strain relationship of main steel for all tested specimens.

3.4 Bond Strength

To estimate the effect of confinement at the lap splice region, the average bond stress (τ) of a spliced bar in tension at the peak capacity of each specimen is calculated assuming that bond is uniformly distributed over the lap length (l_p), based on the test results by the following equilibrium equation:

$$\tau = \frac{f_s d_b}{4\, l_p} = \frac{\varepsilon_s E_s\, d_b}{4\, l_p} \qquad Eq.(1)$$

Where ε_s is the average bar strain (from the strain gauges shown in Figs. (2-3)), E_S is the modulus of elasticity of the bars (E_S= 200 GPa), and the rest of the variables are as defined before. As mentioned, the experimental bar stresses (f_s) of the reinforcement steel of all confined specimens exceeded yielding due to confinement techniques of insufficient lap splice lengths. So, the bond strength of all confined specimens was higher than that of the unconfined specimens as seen in Table 6. Also, using vertical stirrups with UHP-SHCC jacketing in group (II and III) enhanced the bond strength of the spliced bars. Decreasing the spacing between vertical stirrups leads to increasing the bond strength. With respect the lap splice length ($30d_b$), the bond strength was enhanced by up to 110%, 88% and 75% for specimens BS30-60, BS30-72 and BS30-90, respectively. It worth mentioned that, the strengthened specimen BS55-60 with lap splice length according to design codes (55 d_b) doesn't record any increase in bond strength. On the contrary, strengthened specimen BS20-60 having the shortest lap splice length (20 d_b) recorded maximum bond strength. Their bond strength was enhanced by up to 144% compared with its unconfined reference specimen.

Table 6: Bar stresses and bond results of tested specimens.

Specimen	ε_s (MPa)	f_s(MPa)	τ (MPa)	τ / τ_{ctrl}
BC	2500	500	---	---
BC55	2500	500	2.2	---
BC30	1570	314	2.6	---
BC20	1370	274	3.4	---
BS55-60	2845	569	2.5	1.1
BS30-60	3300	660	5.5	2.1
BS30-72	2940	588	4.9	1.8
BS30-90	2800	560	4.6	1.7
BS20-60	3340	668	8.3	2.4

Where f_s: is the experimental bar stress, τ: is the average bond stress of a bar, and τ/τ_{ctrl}: is the bond ratio between the strengthened beam to its control reference specimen.

3.5 Ductility Analysis

Ductility presents the ability of RC elements to sustain significant inelastic deformation prior to collapse. Ductility is a major property for safe design of strengthening structural elements [32]. There are many approaches to estimate the ductility. In this study, two approaches have been utilized in order to estimate the flexural ductility of tested specimens. The first is by calculating the displacement ductility index (μ_Δ) and the second through absorbed energy (μ_E).

3.5.1 Displacement ductility index (μ_Δ)

The displacement ductility index (μ_Δ) is defined as the ratio of the maximum mid-span displacement (Δ_{max}) over the first yield displacement of the specimen (Δ_y) [33] according to Eq. (2):

$$\mu_\Delta = \frac{\Delta_{max}}{\Delta_y} \qquad Eq.(2)$$

Table 7 shows the values of the displacements of all tested specimens at different stages of loading and the corresponding displacement ductility index. As seen in Fig. 10, the ductility ratio of control reference specimen (BC), without lap splice, is controlled by the reinforcing bar yielding. This specimen was designed according to the Egyptian code [31] provisions to be

under-reinforced which is achieved the ratio of ($\mu < \mu_{max}$), so the failure of this specimen was flexural and ductile. On contrary, the displacement ductility index of the control specimen BC55, with sufficient lap splice length, decreased by 80% compared to that of the control reference un-spliced specimen (BC). However, the lap splice length of this specimen was designed according to Egyptian code [31], but this specimen didn't show any ductility. On the same approach, the test results of control specimens BC30 and BC20, with insufficient lap splice lengths, are exceeded due to the premature brittle failure resulted in splitting of spliced reinforcement.

For group (II), the displacement ductility indices showed the effect of confining at different lap splice lengths. All strengthened specimens with STEEL-REINFORCED UHP-SHCC at lap splice region exhibited higher ductility in comparison to their reference specimens. The increasing in displacement ductility are 85%, 80% and 60%, respectively, for BS55-60, BS30-60 and BS20-60. That's indicated that increasing of the lap splice length leads to increasing the tension reinforcement double the cross-sectional area at lap splice region, as well as increasing the number of vertical stirrups along the lap splice length, and that resulted in improvement in ductility. The test results also showed that, the ductility of specimens in group (III), with the same lap splice length (30 db), are much higher than their reference specimen BC30. It can be noticed that strengthening of insufficient lap splices resulted in increasing the ductility indicators by about 80%, 70% and 65% of the control reference un-spliced specimen (BC) for specimens BS30-60, BS30-72, and BS30-90, respectively.

3.5.2 Energy ductility index (μ_E)

The energy ductility index is defined by Thomsen et al. [34] as the ratio between the energy of the specimen at failure (E_u), which represents the area under the entire load–deflection curve up to failure, and the energy of the specimen at yielding load (E_y), which corresponds to the area under the load–deflection curve up to the yielding load according to Eq. (3).

$$\mu_E = \frac{E_u}{E_y} \qquad Eq.(3)$$

For all tested specimens, the failure energy (E_u), elastic energy (E_y), and the energy ductility index (μ_E) are reported in Table 5. Regarding the energy-based ductility, as shown in Fig. 11, the same trend was observed for all tested specimens as that obtained based on the displacement ductility index. All confined specimens in group (II and III) exhibited high energy ductility indicators. With respect the transverse reinforcement ratio embedded in UHP-SHCC jacketing in group (II), the percentage of energy ductility were 85%, 65% and 50% of the control reference un-spliced specimen (BC) for specimens BS55-60, BS30-60, and BS20-60, respectively. Also, with respect the lap splice length ($30d_b$), the energy ductility index increased with increasing the lap splice length. The energy ductility reached to 65%, 55% and 50% of the control reference un-spliced specimen (BC) for specimens BS30-60, BS30-72, and BS20-90, respectively.

Table 7: Ductility indices for test specimens

Specimen	Displacement ductility index (μ_Δ)			Energy ductility index (μ_E)		
	Δ_y (mm)	Δ_{max} (mm)	$\mu_{\Delta=\frac{\Delta max}{\Delta y}}$	E_y (kN m)	E_u (kN m)	$\mu_E = \frac{E_u}{E_y}$
BC1	8.8	67.6	7.7	375.8	4827.4	12.8
BC55	9	15.6	1.7	387.9	860.7	2.2
BC30	**	12.38	**	**	**	**
BC20	**	8.06	**	**	**	**
BS55-60	12.6	82.9	6.6	560.3	6106.3	10.9
BS30-60	12.8	80.4	6.3	680.1	5581.2	8.2
BS30-72	13.7	75.2	5.5	721.8	5124.7	7.1
BS30-90	13.9	73.4	5.2	734.7	4921.2	6.7
BS20-60	15.4	72.2	4.8	733.2	4806.7	6.5

Δ_y: the first yield displacement, Δ_{max}: the maximum displacement, μ_Δ: displacement ductility index = Δ_{max}/Δ_y, E_y: the energy of the specimen at yielding load, E_u: the energy of the specimen at failure, μ_E: energy ductility index = E_u/E_y and **: steel did not yield.

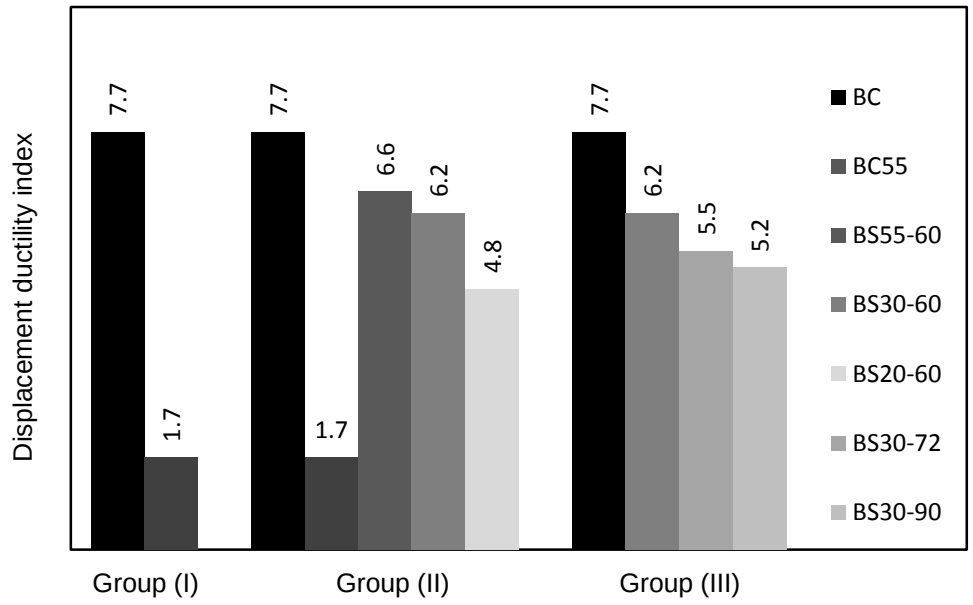

Fig. 10: Displacement ductility index (μ_{Δ}) for all tested specimens.

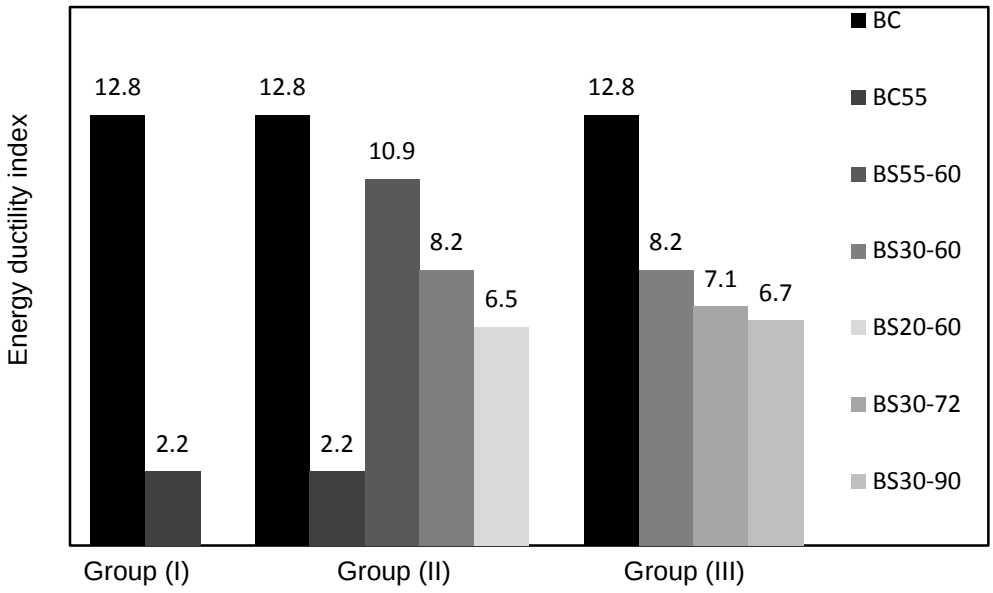

Fig. 11: Energy ductility index (μ_E) values for all tested specimens.

CONCLUSIONS

The experimental programme investigated in this research was designed to evaluate the contribution of confinement for eliminating the splitting failure modes of tension lap splices, thereby allowing flexural reinforcement to develop their full capacities beyond yielding and providing high ductile behavior. Nine RC beams with STEEL-REINFORCED UHP-SHCC strengthening of lap-spliced were experimentally studied. The influence of several parameters such as confinement technique, splice length, and spacing of transverse reinforcement was evaluated. In order to isolate the contribution of confinement technique, no stirrups were used in lap splice region for tested specimens.

Based on the experimental investigation, the following conclusions and recommendations can be estimated:

- The failure of the un-spliced control specimen was flexural and ductile. In contrast, the spliced control specimens failed in a brittle manner due to splitting of main steel and the behavior of all these specimens lacks ductility.
- Compared to the reference un-spliced specimen (BC), the spliced specimen (BC55), with sufficient lap splice length, the tension reinforcement reached the yield strain. Nevertheless, a brittle failure due to splitting of main steel was occurred. On the other hand, the confined specimen with the same lap splice length(BC55-60) didn't report any increase in loads but its mode of failure changed to flexural failure with yielding of main steel.
- For splices confined by UHP-SHCC jacketing with embedded vertical stirrups at lap splice region, the mode of failure changed from splitting failure to flexural failure.
- Using of strengthening technique based on STEEL-REINFORCED UHP-SHCC on lap splice length lead to an increase in the ultimate load and deflection and resulted in improvement in ductility.
- As the amount of transverse reinforcement in strengthening layer at the splice region increased, more ductility provided to the mode of failure.
- Based on the test results, whilst unconfined spliced specimens failed prematurely due to cover splitting, using of UHP-SHCC jacketing with embedded vertical stirrups as a strengthening technique enhanced the bond strength of the spliced bars and resulted in a ductile behavior.

REFERENCES

1. Lee JK, (2016) Bonding behavior of lap-spliced reinforcing bars embedded in ultra-high strength concrete with steel fibers. KSCE Journal of Civil Engineering 20(1):273-281
2. Rao GA, Reddy SP, Eligehausen R, (2012) Prediction of analytical bond strength of lap splices in tension. Proceedings of the 9th International Conference on Fracture Mechanics of Concrete and Concrete Structures, FraMCoS-9 V. Saouma, J. Bolander and E. Landis (Eds).
3. Orangun CO, Jirsa JO, Breen JE (1977) Reevaluation of test data on development length and splices. ACI journal, 74(3):114-122
4. Darwin D, Tholen ML, Idun EK, Zuo J (1996a) Splice strength of high relative rib area reinforcing bars. ACI Structural Journal, 93(1):95-107
5. Zuo J, Darwin D, (2000) Splice strength of conventional and high relative rib area bars in normal and high-strength concrete. ACI Structure Journal, 97(4):630–641
6. Mabrouk RTS, Mounir A (2018) Behavior of RC beams with tension lap splices confined with transverse reinforcement using different types of concrete under pure bending. Alexandria Engineering Journal 57(3), 1727-1740
7. Tepfers R (1973) A theory of bond applied to overlapping tensile reinforcement splices for deformed bars. Publication 73:2, Division of Concrete Structures, Chalmers University of Technology, Goteborg, Sweden, 328 pp
8. Darwin D, Graham EK (1993a) Effect of deformation height and spacing on bond strength of reinforcing bars. ACI Materials Journal, 90(6):646-657
9. Darwin D, Graham EK (1993b) Effect of deformation height and spacing on bond strength of reinforcing bars. SL Report 93-1, University of Kansas Center for Research, Lawrence, Kans., Jan., 68 pp.
10. Pandurangan K, Kothandaraman S, Sreedaran D (2010) A study on the bond strength of tension lap splices in self compacting concrete. Materials and Structures, 43:1113–1121
11. Abdel-Kareem AH, Abousafa H, El-Hadidi OS (2013) Effect of transverse reinforcement on the behavior of tension lap splice in high-strength reinforced concrete beams. International Journal of Civil, Environmental, Structural, Construction and Architectural Engineering, 7(12): 989- 996
12. ACI 318-05, Building Code Requirements for Structural Concrete and Commentary, American Concrete Institute, Michigan, 2005
13. Tarabia AM, Shoukry MS, Diab MA (2010) Improving the behavior of reinforced concrete beams with lap splice reinforcement. Challenges, Opportunities and Solutions in Structural

Engineering and Construction, Proceedings of the 5th Intnl. Struct. Engrg. and Constrn. Conf., Las Vegas, Sept 22-25, CRC Press/Balkema, pp 81-86

14. Rakhshanimehr M, Esfahani MR, Kianoush MR, Mohammadzadeh BA, Mousavi SR (2014) Flexural ductility of reinforced concrete beams with lap-spliced bars. Can. J. Civ. Eng., 41: 594–604
15. Helal Y, Garcia R, Pilakoutas K, Guadagnini M, Hajirasouliha I (2016) Strengthening of short splices in RC beams using Post-Tensioned Metal Straps. Materials and Structures, 49:133–147
16. Harajli MH (2008) Seismic behavior of RC columns with bond-critical regions: criteria for bond strengthening using external FRP jackets. J. Compos. Constr. 12(1):69–79
17. Priestley MJN, Seible F (1995) Design of seismic retrofit measures for concrete and masonry structures. Constr Build Mater 9(6):365–377
18. Sause R, Harries KA, Walkup SL, Pessiki S, Ricles JM (2004) Flexural behavior of concrete columns retrofitted with carbon fiber-reinforced polymer jackets. ACI Struct J 101(5):708–716
19. Garcia R, Helal Y, Pilakoutas K, Guadagnini M (2014) Bond behaviour of substandard splices in RC beams externally confined with CFRP. Construction and Building Materials, 50:340–351
20. Hamad B S, Rteil A A, Soudki K A (2004) Bond strength of tension lap splices in high-strength concrete beams strengthened with glass fiber reinforced polymer wraps. Journal of composites for construction,8:14-21
21. Dagenais MA, Massicotte B (2015) Tension lap splices strengthened with ultrahigh-performance fiber-reinforced concrete. Journal of Materials in Civil Engineering, 27(7): 04014206
22. Elnagar AB, Baraghith AT, Afefy HA, Mahmoud MH (2017) Effect of Internal Reinforcement on the Tensile Characteristics of the UHP-SHCC Material, Proceedings of the International Conference on Advances in Structural and Geotechnical Engineering, ICASGE'17, Hurghada, Egypt. Faculty of Engineering, Tanta University, Egypt, 27-30 March
23. Li, V. C., (1993), "From micromechanics to structural engineering: the design of cementitious composites for civil engineering applications" JSCE Journal of Structural Mechanics and Earthquake Engineering, Vol. 10, pp. 37-48.
24. Kunieda, M., Denarie, E., Bruhwiler, E., Nakamura, H., (2007), "Challenges for strain hardening cementitious composites-deformability versus matrix density" Proc. of the 5th Int. RILEM workshop on HPFRCC, pp. 31-38.
25. Kamal, A., Kunieda, M., Ueda, N., Nakamura, H., (2008), "Evaluation of crack opening performance of a repair material with strain hardening behavior" Cement and Concrete Composites, Vol. 30, No. 10, pp. 863–871.
26. Kunieda M, Ueda N, Nakamura H, Tamakoshi T., (2009), "Development of spraying technique for UHP-SHCC" Proc. of the Concrete Structure Scenarios Vol. 9, pp. 349–354. Hussein M, Kunieda M, Nakamura H (2012) Strength and ductility of RC specimens strengthened with steel-reinforced strain hardening cementitious composites. Cement & Concrete Composites 34:1061–1066
27. Kunieda M, Hussein M, Ueda N, Nakamura H (2010) Enhancement of crack distribution of UHP-SHCC under axial tension using steel reinforcement. Journal of Advanced Concrete Technology, Vol.8, No.1, pp. 49-57
28. Atta AM, (2012), "Evaluation of the efficiency of UHP-SHCC specimens in flexure under external pre-stressing (comparative study)", Magazine of Concrete Research, 64(1):43-54
29. Khalil AE, Etman E, Atta A, Essam M (2017) Behavior of RC specimens strengthened with strain hardening cementitious composites (SHCC) subjected to monotonic and repeated loads. Engineering Structures, 140:151–163
30. Kunieda M., Hussein M., Ueda N. and Nakamura H. (2010): Fracture behavior of steel reinforced UHP-SHCC under axial tension, Fracture Mechanics of Concrete Structures, Proceedings FRAMCOS-7, pp.1557-1564.
31. ECP 203-2007, Egyptian Building Code for Structural Concrete Design and Construction, Ministry of Housing, 2007.

32. Afefy HM, Mahmoud MH (2014) Structural performance of RC slabs provided by pre-cast ECC strips in tension cover region. Construction and Building Materials 65:103–113
33. Bonaldo E, Oliveira de Barros JA, Lourenço PB (2008) Efficient strengthening technique to increase the flexural resistance of existing RC slabs. J Compos Constr; 12:149–59.
34. Thomsen HH, Spacone E, Limkatanyu S, Camat G (2004) Failure mode analysis of reinforced concrete specimens strengthened in flexure with externally bonded fiber-reinforced polymers. J Compos Constr; 8:123–31.
35. Eurocode 2. 1992. Design of concrete structures - Part 1-1: General rules and rules for buildings, 2003.
36. CSA-A23.3-04. 2004. Design of concrete structures. CAN/CSA A23.3, Canadian Standards Association (CSA), Rexdale, Ont.